



**HAL**  
open science

# Impact of asymmetrical heating on the uncertainty propagation of flow parameters on wall heat transfers in solar receivers

Martin David, Adrien Toutant, Françoise Bataille

## ► To cite this version:

Martin David, Adrien Toutant, Françoise Bataille. Impact of asymmetrical heating on the uncertainty propagation of flow parameters on wall heat transfers in solar receivers. *Applied Thermal Engineering*, 2021, 199, pp.117547. 10.1016/j.applthermaleng.2021.117547 . hal-03394514

**HAL Id: hal-03394514**

**<https://univ-perp.hal.science/hal-03394514>**

Submitted on 23 Feb 2023

**HAL** is a multi-disciplinary open access archive for the deposit and dissemination of scientific research documents, whether they are published or not. The documents may come from teaching and research institutions in France or abroad, or from public or private research centers.

L'archive ouverte pluridisciplinaire **HAL**, est destinée au dépôt et à la diffusion de documents scientifiques de niveau recherche, publiés ou non, émanant des établissements d'enseignement et de recherche français ou étrangers, des laboratoires publics ou privés.

## Highlights

### **Impact of asymmetrical heating on the uncertainty propagation of flow parameters on wall heat transfers in solar receivers**

Martin David, Adrien Toutant, Françoise Bataille

- A heat transfer correlation is used to determine wall heat flux sensitivity.
- Uncertainty propagation in symmetric and asymmetric heating are compared.
- The general uncertainty management procedure provides reliable results.
- The bulk temperature and the cold wall temperature require accurate measurements.
- The uncertainty propagation is very dependent on the location in the solar receiver.

# Impact of asymmetrical heating on the uncertainty propagation of flow parameters on wall heat transfers in solar receivers<sup>\*</sup>

Martin David<sup>a</sup>, Adrien Toutant<sup>a,\*</sup> and Françoise Bataille<sup>a</sup>

<sup>a</sup>Laboratoire PROMES-CNRS (UPR 8521), Université de Perpignan via Domitia, Technosud-Rambla de la thermodynamique, 66100 Perpignan – France

---

## ARTICLE INFO

### Keywords:

heat transfer  
correlation  
sensitivity analysis  
uncertainties

## ABSTRACT

Uncertainties may skew the understanding of experiments or numerical simulations results. The impact of the flow parameters uncertainties of measurement on wall heat flux is investigated in a non-isothermal turbulent channel flow. A heat transfer correlation dedicated to gas-pressurized solar receivers of concentrated solar tower power is used. Both symmetric and asymmetric heating conditions are tested. A sensitivity study is performed. The effects of the wall and bulk temperatures are analyzed in a large bulk-to-wall temperature ratio range. The Guide to the expression of Uncertainty in Measurement (GUM) is applied and provides an analytical expression of the uncertainty propagation. Assuming the quasi-normality and quasi-linearity of the studied function, this method provides approximate results. The results obtained following the methodology described in the GUM are then compared to the direct computation of the wall heat flux with altered temperatures. The study shows a dependence of the high heat flux estimation to some temperature variations, highlighting the necessity of accurate measurements. This is particularly salient in the end region of the solar receiver, *i.e.* when the bulk and the wall temperature are close. The GUM produces very satisfying estimations in the symmetric conditions and quite satisfying estimations in the asymmetric conditions. This study shows that the accuracy of measurement devices should be adapted according to their location in the solar receiver.

---

## 1. Introduction

In applied engineering devices, there are many possible sources of uncertainty: measurement with finite instrument resolution, personal bias in reading analog instruments, inadequate knowledge of the effects of environmental conditions on the measurement [1]. The committed errors should be put into perspective with a sensitivity analysis. They may become very problematic when moving from principles to a functioning system. Indeed, while some devices are poorly affected by parameter variations, some are very sensitive to specific parameters. For example, in gas turbines the wall temperature variation greatly affects the lifetime of the components: it is generally accepted that a variation of 20 K in the metal reduces the life of the components by 50% [2]. Uncertainties may skew the understanding of the results of experiments or numerical simulations. For that reason, several authors propose methods to bring uncertainties out. Some studies dealing with uncertainties in the fields of fluid me-

chanics and heat transfers are addressed below. Oliver *et al.* [3] address two major sources of uncertainty in statistics computed from Direct Numerical Simulation (DNS): finite sampling error and discretization error. They propose a systematic and unified approach to estimate these two uncertainty sources when resolving the Navier–Stokes equations. A Bayesian extension of the standard Richardson extrapolation that accounts for both statistical uncertainty and prior information is formulated. Phillips and Roy [4] investigate the accuracy of various Richardson extrapolation-based discretization error and uncertainty estimators for problems in computational fluid dynamics. The Richardson extrapolation consists in using two solutions on systematically refined grids to estimate the exact solution to partial differential equations. This method is only applicable when the grids are sufficiently fine. Carneval *et al.* [5] propose a stochastic method to predict heat transfer using Large Eddy Simulation (LES). It consists in coupling a classical uncertainty quantification to LES in a duct with pin fins. The authors demonstrate that the uncertainties related to the unknown conditions, named aleatoric uncertainties, and those related to the physical model, named epistemic uncertainties, are strongly interconnected. Menberg *et al.* [6] investigate three methods for sensitivity analysis in relation to dynamic, high-order, non-linear behavior and the level of uncertainty in building energy models. Prediction of uncertainties in heat transfer coefficient determination is a commonly studied topic. For instance, a large number of works addresses the uncertainty prop-

---

<sup>\*</sup> This document is the results of the research project funded by the Occitania region.

\*Corresponding author

martin.david@promes.cnrs.fr (M. David);  
adrien.toutant@univ-perp.fr (A. Toutant);  
francoise.bataille@promes.cnrs.fr (F. Bataille)  
ORCID(s): 0000-0001-5213-8712 (M. David);  
0000-0002-7156-1732 (A. Toutant)

agation when estimating the convection coefficients in a wide spectrum of convective heat transfer processes with the Wilson plot method. Uhía *et al.* [7] detail the application of the Guide to the expression of Uncertainty in Measurement (GUM) [1] for calculating the uncertainty associated with experimental heat transfer data obtained thanks to the Wilson plot method. They illustrate their work by applying the GUM to the specific process of condensation of R-134a on a horizontal smooth tube. The impact of the uncertainty of

## Nomenclature

Err	relative error
L	hydraulic diameter [m]
Nu	Nusselt number based on hydraulic diameter
Pr	Prandtl number
Re	Reynolds number based on hydraulic diameter
Ri	Richardson number based on hydraulic diameter
$T_m$	mean wall temperature [K]
T	temperature [K]
Y	flow parameter

### Greek symbols

$\Delta$	uncertainty
$\lambda$	thermal conductivity [W/(K.m)]
$\phi$	heat flux [kW/m <sup>2</sup> ]

### Subscripts and superscripts

alt	altered
asy	asymmetric heating conditions
b	bulk
cor	referring to the correlation
c	cold wall
h	hot wall
max	maximum
m	mean
ref	reference
sim	referring to the simulation
sym	symmetric heating conditions
w	wall
$\bar{w}$	opposite wall

measurements is discussed on the basis of two normalized coefficients proposed by Coleman and Steele [8]: the uncertainty magnification factor (UMF) and the uncertainty percentage contribution (UPC). The effects of the temperature interference on the results obtained using the Wilson plot technique are also investigated by Wójs and Tietze [9]. The authors highlight the importance of using adequate experimental data to obtain reliable results.

The uncertainty propagation can be quantified with probabilistic and deterministic methods. The Monte Carlo approach rely on repeated random sampling. It is very commonly used in engineering [10–16]. The

methodology has many advantages: it is a general and powerful technique that can be applied to non-linear problems. However, the computational cost of Monte Carlo simulation can easily become prohibitive [17]. Taler [18] details the calculation of the indirect measurement uncertainty using the rule formulated by Gauss for the uncertainty propagation. The non-linear least squares method used to estimate parameters and indirectly determined quantities are described and several examples of uncertainty determination of measured parameters involved in heat transfer correlations are presented. Functional expansion-based methods such as the arbitrary polynomial chaos expansion [19], Karhunen–Loève expansion [20], and Neumann expansion [21] can also be used for uncertainty quantification. The Guide to the expression of Uncertainty in Measurement (GUM) provides a local expansion-based method involving the Taylor expansions. It gives general rules for evaluating and expressing uncertainty in measurement that are intended to be applicable to a broad spectrum of measurements. It is considered as a general cross-disciplinary standard, applicable to all fields. Furthermore, it produces an analytical expression of the error. The GUM framework assumes the quasi-linearity and the quasi-normality of the studied function. The linear approximation of the function has to be close to the function in the uncertainty range. The GUM method is particularly advantageous when dealing with reasonable input variability and outputs that do not express high non-linearity. For these reasons, this method is selected to study the sensitivity of the wall heat flux to flow parameters. The GUM framework is detailed in [1]. Studying convective heat transfer, Håkansson [22] notices some incoherence in the literature when regarding heat transfer coefficient values. Using the GUM, he points out that several methods used to determine the heat transfer coefficient are very dependent on the accuracy of measurements. This could be responsible for the various results obtained in the literature.

Heat transfer correlations are widely used in engineering field to estimate wall heat flux of complex devices such as automobile radiators [23], heat exchangers [24–26], and solar receivers of concentrated solar power tower [27]. Correlations allow the estimation of the heat transfer within, generally, 10% to 20% of error [27–32]. This accuracy is usually acceptable for pre-dimensioning. However, it is necessary to consider the uncertainty of measurements and their propagation to estimate an error range associated with the heat flux prediction. Correlation may also be useful to quantify the heat transfer sensitivity to parameters. Table 1 gives the major results of some studies investigating uncertainty propagation.

To the author's knowledge, there is no study addressing wall heat flux sensitivity in the operating conditions of solar receivers. In this paper, a correlation developed for both symmetrically and asymmetrically

**Table 1**  
Major results of some literature papers dealing with uncertainty propagation.

Authors	Topic	Major results
Driscoll and Landrum [33]	Uncertainty on heat transfer correlations for fuel in copper tubing. They quantify the influence of uncertainties on the engine design.	The overall uncertainty on the Nusselt number can reach 36%. The magnitude of the uncertainty values and their impact on engine design parameters highlights the importance of mitigating the Nusselt number uncertainties.
Scariot <i>et al.</i> [34]	Influence of the uncertainty of measurements on the fluid temperature and enthalpy in carbon dioxide tube flow using heat transfer correlations.	Results shows that the uncertainty propagation is significantly influenced by the local conditions. They state that the difficulty to predict experimental data from correlations is due to the observed uncertainty amplification. In the worst case, the uncertainties on the enthalpy range from -7% to +15%, considering that the correlation has a 10% uncertainty under such conditions. These uncertainties are significantly increased if the accuracy of the correlation decreases.
Dimassi and Dehamni [35]	Experimental thermal analysis of a Trombe wall	Uncertainties of thermal heat fluxes can reach 4.8% despite small uncertainties on the temperature, velocity, radiation coefficient, and convection coefficient measurements.
Sciacchitano and Wieneke [36]	PIV uncertainty propagation	The uncertainty of the vorticity is estimated typically within 5–10% accuracy, time-averaged velocities are accurate within 5%. The Reynolds stresses are more difficult to estimate and the PIV gives a prediction within 10%.
Paudel and Hostikka [37]	Stochastic simulations of a compartment fire with Fire Dynamic Simulation.	The results show that the prediction uncertainty for both gas phase and solid phase temperature is accurate within 10%.
Zhao <i>et al.</i> [38]	Uncertainty and sensitivity analysis of flow parameters for transition models on hypersonic flows.	Uncertainties on heat flux and skin friction coefficient distribution, as well as uncertainties on the Stanton number, and the onset and length of the transition zone are investigated. The uncertainty results quantitatively verify that the transition zone is greatly sensitive to changes in flow parameters. The transition length and onset are estimated within 10% of uncertainty.

heated turbulent channel flow is used to quantify the propagation of the uncertainties of the flow parameters on the wall heat fluxes. Firstly, the used correlation is presented in Section 2. The sensitivity of the heat fluxes to flow parameters is analyzed under symmetric heating conditions and in the working conditions of gas-pressurized solar receivers of concentrated solar power tower (Section 3). Then, in Section 4, the results obtained by the GUM applied to the correlation are compared to the direct computation of the wall heat fluxes with the same variations of the input parameters in both heating conditions. The entire applicable range of the correlation in terms of bulk-to-cold wall temperature is investigated.

## 2. Heat transfer correlation for turbulent channel flow

The correlation proposed by David *et al.* [27] aims to estimate the heat transfer in the working conditions of gas-pressurized solar receivers. This technology is still in the research stage. Numerous geometries are investigated in the literature including tubes [39], channels with vortex generators [40, 41], and thin channels [42, 43]. In the present study, we focus on this last type of

gas-pressurized solar receiver. A bi-periodic channel is used to model the geometry. The correlation has been established thanks to 70 Thermal-Large Eddy Simulations, constituting a consequent and reliable database. In those simulations, the Navier-Stokes equations are solved under the low Mach number approximation. The coupling between velocity and temperature is considered. The thermal dilatation is taken into account. The density is linked to the temperature variations thanks to the ideal gas-law. The gravity force is not taken into account since its impact is negligible in the working conditions. Indeed, the Richardson number is about  $10^{-5}$ . The correlation is obtained for fully developed flows. The simulations are performed in a bi-periodical channel. To lower the fluid temperature, a source term is introduced in the energy equation. It allows to maintain a constant bulk temperature. Hence, this temperature corresponds to the average of the fluid temperature along the wall-normal direction. The small turbulent scales are not solved in LES. Their effects on bigger turbulent structures are considered thanks to the Anisotropic-Minimum-Dissipation (AMD) model. This model showed a good agreement with DNS in similar conditions [44–46]. The proposed correlation is given

by:

$$\text{Nu}_w^{\text{asy}} = 0.024 \text{Re}_b^{0.8} \text{Pr}_b^{0.4} \left( \frac{T_w}{T_b} \right)^{-0.9} \left( \frac{T_w}{T_w - T_b} \right)^{1.4 \left( 1 - \frac{T_w}{T_m} \right) \frac{T_b}{T_w}}, \quad (1)$$

with  $T_m = (T_h + T_c)/2$ .

A term accounting for asymmetric heating conditions is included in the equation to reproduce the heat transfers at both walls taking into account the respective effects of one on this other. This term involves flow parameters in the exponent. The singularity of the Nusselt number, observed when the bulk temperature (defined as the average fluid temperature) tends towards the cold wall temperature and explained by Nield in [47], is reproduced thanks to the difference of temperature at the denominator of the asymmetric group. This term, accounting for asymmetric condition, is equal to 1 in the case of symmetric heating conditions leading to the correlation presented below:

$$\text{Nu}_w^{\text{sym}} = 0.024 \text{Re}_b^{0.8} \text{Pr}_b^{0.4} \left( \frac{T_w}{T_b} \right)^{-0.9}. \quad (2)$$

The proposed correlation is studied in the commonly encountered working conditions of heat exchangers and solar receivers. The validity domain of the correlation in terms of Reynolds number and temperature ranges is given in Table 2. The wall temperatures vary from 293 K to 1300 K. The fluid temperature ranges from 342 K to 1237 K, Prandtl number is between 0.76 and 3.18, and heat fluxes vary from 4 kW/m<sup>2</sup> to 578 kW/m<sup>2</sup>.

**Table 2**

Applicable domain of the correlation.

Symmetric heating	Asymmetric heating
12000 < Re <sub>b</sub> < 177000	10600 < Re <sub>b</sub> < 145000
0.47 < T <sub>b</sub> /T <sub>w</sub> < 0.99	1.1 < T <sub>h</sub> /T <sub>c</sub> < 2.0
	0.63 < T <sub>b</sub> /T <sub>c</sub> < 0.95
	0.44 < T <sub>b</sub> /T <sub>h</sub> < 0.85

An overview of the point distribution is given in this paragraph. The values are given indifferently for both types of heating. The Reynolds number ranges from 10600 to 177000. 25 different values of Reynolds number are covered with a mean step of 6400. The Prandtl number is between 0.76 and 3.18. The values taken by the Prandtl number are dependent of the temperatures. Most of the points are around 3.1, 2.6, 1, and 0.8. The hot wall temperature is between 586 K and 1300 K. The covered values are: 586 K, 700 K, 810 K, 900 K, 1100 K, and 1300 K. The cold wall temperature is between 293 K and 1300 K. It takes the following values: 293 K, 500 K, 700 K, 810 K, 900 K, 1100 K, and 1300 K.

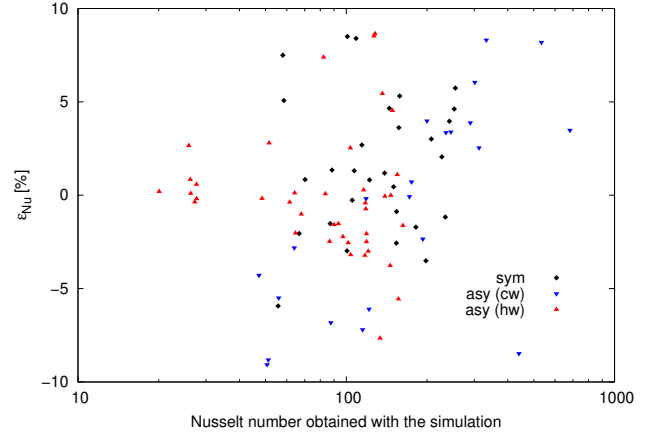


**Figure 1:** Relative error on the Nusselt number obtained with the heat transfer correlation as function of the Nusselt number obtained by the simulation.

The bulk temperature is between 461 K and 1236 K. The range is homogeneously covered. There are several bulk temperature points in every 50 K interval.

The Nusselt numbers obtained with the correlation proposed by David *et al.* [27] are plotted against the Nusselt numbers obtained with the numerical simulations in Figure 1. The relative error on the Nusselt number is obtained as follows:

$$\epsilon_{\text{Nu}} = \frac{\text{Nu}_{\text{cor}} - \text{Nu}_{\text{sim}}}{\text{Nu}_{\text{sim}}}. \quad (3)$$

Black dots stand for the Nusselt number obtained under symmetric heating conditions. Red dots, respectively blue dots, account for the Nusselt obtained at the hot wall, respectively cold wall, under asymmetric heating conditions. The Nusselt number range is between 20 and 680. The results show that all the points are within the 10% error range. A detailed analysis of the data shows that more than three-quarters of the results are in the error bound 5%. The determination coefficient is 0.993. The mean error is 0.29% and the standard deviation is 4.1%.

In the following, the wall heat fluxes are computed using the Nusselt numbers obtained with the correlation thanks to equation presented below:

$$\phi_w = \frac{\lambda_w (T_w - T_b) \text{Nu}_w}{L}. \quad (4)$$

Figure 2 aims to give an overview of the wall heat flux behavior depending on the ratio between bulk temperature and the average of both wall temperatures in both heating conditions. It permits linking the heat flux uncertainties presented in Section 4 to the value of the reference heat flux. The Reynolds number and the wall temperatures used to obtain Figure 2 are those referenced in Table 3 for the symmetric heating case and those referenced in Table 5 for the asymmetric heating case. The bulk temperature varies between

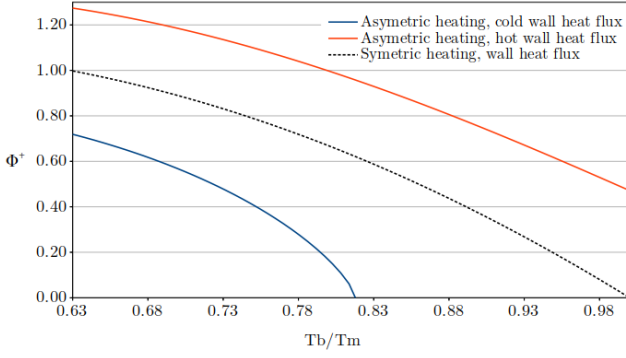


**Figure 2:** Normalized wall heat fluxes as function of the ratio between bulk temperature and the average of both wall temperatures. The wall temperatures are 1300 K and 900 K in the case of asymmetric heating. They are of 1100 K in the case of symmetric heating. The bulk temperature and the Reynolds number are respectively 700 K and 60 000.

700 K and 1100 K. Hence, this figure is valid for a fixed Reynolds number of 60 000 and fixed wall temperatures of 1100 K under symmetric heating condition or 900 K and 1300 K under asymmetric heating conditions. The wall heat fluxes are normalized with the following equation:

$$\phi^+ = \frac{\phi_w(T_b/T_m)}{\phi_{w, \max}^{\text{sym}}}, \quad (5)$$

where  $\phi_{w, \max}^{\text{sym}}$  corresponds to the maximum wall heat flux obtained under symmetric heating and  $\phi_{w, \max}^{\text{sym}} = 198 \text{ kW/m}^2$ . This maximum wall heat flux obtained under symmetric heating is reached for a Reynolds number of 60 000, a Prandtl number of 0.87, a bulk temperature of 700 K, and wall temperature of 1100 K. The ratio  $T_b/T_m$  into brackets is a functional expression. The wall heat fluxes are decreasing with the increase of the temperature ratio. For the asymmetric case, the cold wall heat flux is rapidly diminishing and became equal to zero when the bulk and cold wall temperatures are the same. On the hot side, the normalized heat flux is slowly decreasing and reaches 0.45 for a ratio between bulk temperature and the average of both wall temperatures of 1. In the symmetric heating conditions, the wall heat flux is moderately diminishing.

### 3. Wall heat flux sensitivity

Studying the sensitivity of wall heat flux with a correlation is an interesting approach to highlight the influence of each parameter. It gives the measurement accuracy necessary to provide a reliable prediction of the wall heat fluxes. In the applicable domain of the correlation, the estimated wall heat flux sensitivity reflects the physic behavior. A high temperature sensitivity calculated with the correlation means that the physical wall heat flux is greatly impacted by this parameter. In Subsections 3.1 and 3.2, the wall heat flux

is computed thanks to the direct application of the correlation. A routine is used to compute the reference wall heat flux and the altered wall heat flux thanks to the correlation. The altered wall heat flux is calculated by altering a single flow parameter from -10% to 10% of its reference value by step of 0.5%. For each step, the ratio between the reference and the altered wall heat flux is computed and reported in Figures 3 and 5.

#### 3.1. Symmetric heating conditions

Firstly, the sensitivity of the wall heat fluxes is studied in symmetric heating condition. These conditions are summarized in Table 3.

**Table 3**

Studied conditions in the symmetric heating case.

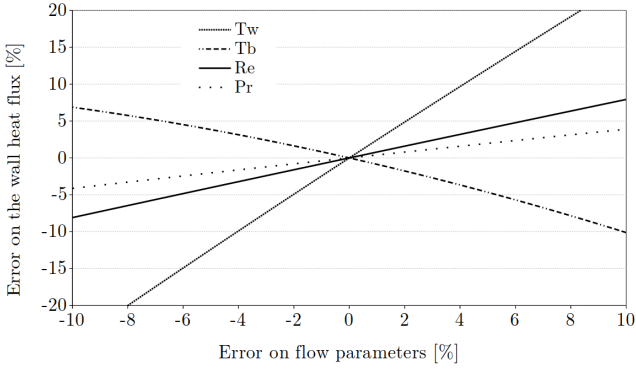
$Re_b$	$Pr_b$	$T_h$ [K]	$T_c$ [K]	$T_b$ [K]
60 000	0.87	1100	1100	700

Figure 3 exposes the error on the wall heat fluxes depending on the error committed on various flow parameters in the symmetric heating conditions presented in Table 3. The propagation of the error committed on the measurements of the wall temperature, the bulk temperature, the Reynolds number, and the Prandtl number are studied. The error on the wall heat flux is computed as follows:

$$\text{Err}_\phi = \frac{\phi(Y_{\text{alt}}) - \phi(Y_{\text{ref}})}{\phi(Y_{\text{ref}})}, \quad (6)$$

where  $Y_{\text{alt}} = Y_{\text{ref}} + x\%$  with  $x$  ranging between -10% and 10%. The errors on flow parameters are defined in the same way that the error on the wall heat flux and described by equation 3.1. All the temperatures are expressed in degree Kelvin. The results show that uncertainties on wall temperature are amplified. They induce an important error on the wall heat flux. The bulk temperature and Reynolds number estimations are less impacting but remain consequent. The wall heat flux error is mitigated when compared to the error on the Prandtl number. Indeed, the wall heat flux error is in the 5% error range. The ranking of the parameters in terms of influence is independent of the uncertainty of measurement.

Figure 4 presents the slope of the error propagation for uncertainties relative to the wall and bulk temperatures. The curves observed in Figure 3 are approximated by straight lines thanks to the generalized least-squares method. Four wall temperatures are investigated. The wall temperature increases from 700 K to 1300 K. In each case, the bulk temperature is 200 K below the wall temperature. The investigated cases are listed in Table 4. The error propagations concerning the Reynolds number and the Prandtl number are not affected by the thermal conditions that is why they are not plotted in this figure. The results show that the



**Figure 3:** Error on the wall heat fluxes depending on the error committed on various flow parameters for symmetric heating conditions. The results are obtained with the conditions listed in Table 3.

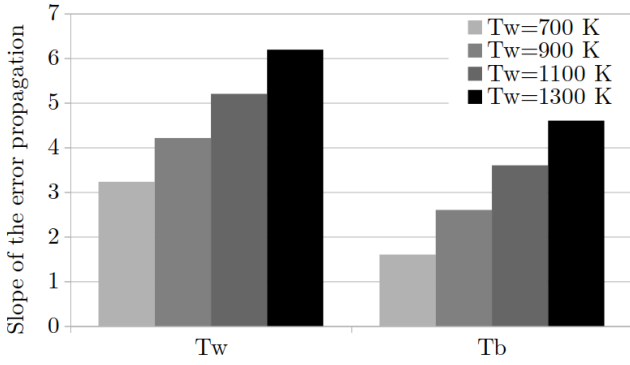


**Figure 4:** Slope of the error propagation in absolute value for wall and bulk temperatures. Four wall temperatures are investigated, see Table 4. The bulk Reynolds number is 60 000 for all the tested cases.

slope of the error propagation increases linearly with the wall temperature. In the studied cases, the slope of the error propagation corresponding to the wall temperature is higher than the slope of the error propagation of the bulk temperature.

**Table 4**

List of the tested cases in Figure 4.

$T_w$ [K]	$T_b$ [K]	$T_b/T_w$
700	500	0.71
900	700	0.78
1100	900	0.82
1300	1100	0.85

### 3.2. Asymmetric heating conditions

The sensitivity of the wall heat fluxes is studied in the typical working conditions of gas-pressurized solar receivers [40]. Asymmetric heating is due to the fact that one wall is irradiated by the concentrated sunlight and the opposite wall is insulated on the exterior face of the solar receiver (the one which is in contact

with ambient air). The flow temperature is increasing as the fluid moves forward. These conditions are summarized in Table 5. In the following, the insulated wall is denoted as the "cold wall" for practical reasons. Nonetheless, in this study and in classical working conditions of solar receiver, for a given axial distance from the inlet, the mean fluid temperature is lower than the insulated wall temperature. Indeed, the "cold wall" is indirectly heated by the concentrated sunlight thanks to the radiations of the hot wall.

**Table 5**

Studied conditions in the asymmetric heating case.

$Re_b$	$Pr_b$	$T_h$ [K]	$T_c$ [K]	$T_b$ [K]
60 000	0.87	1300	900	700

The impact of the error, committed on various flow parameters, on the wall heat fluxes is plotted in Figure 5. The results are obtained in the working conditions discussed in Table 5. The bulk-to-cold wall temperature ratio is 0.78, reproducing the working conditions observed in the middle of the solar receiver [40]. As expected, the results show that the uncertainties on the cold wall temperature (respectively hot wall temperature), induce the biggest uncertainties on the cold wall heat flux (respectively hot wall heat flux). The cold wall heat flux is highly sensitive to the bulk temperature. The hot wall is less sensitive to the fluid temperature. These different behaviors are due to the asymmetric heating of the fluid. Since the bulk temperature is closer to the cold wall temperature than the hot wall temperature, the uncertainties are bigger when estimating the cold wall heat flux but they are associated with smaller heat transfers. The opposite wall temperatures also have an impact on the wall heat fluxes, even if it is much smaller than the effect of the concerned wall temperature. The propagation of the uncertainties on the bulk Reynolds number is similar to the propagation of the uncertainties on the hot wall temperature when studying the cold wall heat flux. The error committed on the Prandtl number has low impact on the heat flux prediction. For the four last discussed parameters and regarding the impact of the cold wall temperature on the hot wall heat flux, the propagation of the error on the heat flux is mitigated compared to the error on these parameters. For instance, an overestimation of the Reynolds number of 10% leads to an error of 8%. Notice that the propagation of bulk temperature uncertainties is not symmetric. An overestimation of 10% of the bulk wall temperature induces 20% of error on the cold heat flux, whereas an under-estimation of 10% of this temperature conducts to an error of 13% on the heat flux. The ranking of the parameters in terms of influence is independent of the uncertainty of measurement.

In Figure 6, the curves observed in Figure 5 are ap-

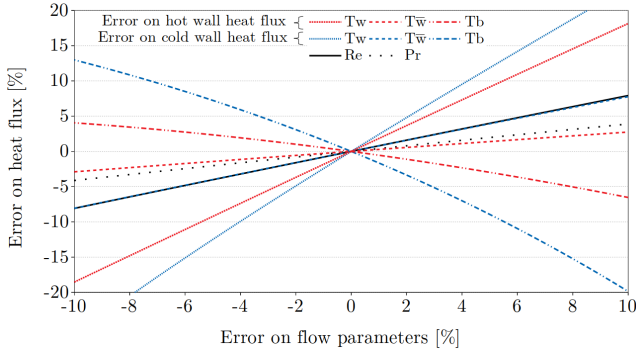


**Figure 5:** Error on the wall heat fluxes depending on the error committed on various flow parameters depending on the bulk-to-cold wall temperature ratio. The results are obtained with the conditions listed in Table 5.

proximated by straight lines thanks to the generalized least-squares method. The slope of the heat flux error is computed for each flow parameter. The coefficient of determination is superior to 0.999 for all the parameters except the bulk temperature, for which it is 0.979 in the most unfavorable case. Three bulk temperatures, corresponding to three locations in the solar receiver, are investigated. The left graph displays the slope of the error propagation on the hot wall heat flux and the right graph gives information on the cold wall heat flux. The slope of the error propagation of the wall and bulk temperatures increases with the bulk temperature. The errors of the Reynolds number and the Prandtl number are independent of the bulk temperature. As observed in Figure 5, the slope of the errors is bigger on the cold wall heat flux than on the hot wall heat flux. Furthermore, their increase soars when the bulk temperature becomes close to the cold wall temperature. So, the measurement of the flow parameter should be adapted to the location in the solar receiver in order to keep a constant uncertainty on the wall heat fluxes.

In Figure 7, four couples of wall temperatures are investigated. The hot wall temperature increases from 700 K to 1300 K. In each case, the cold temperature is 200 K below the hot wall temperature. The bulk temperature is chosen so that it is 250 K below the mean of hot and cold wall temperatures, see Table 6. The results show that the cold wall heat flux is more sensitive than the hot wall. The slope of the error propagation increases linearly with the temperatures as observed in Figure 4. The slope inclination of the error propagation of the bulk temperature steepen faster with the increase of the wall temperature than the one of the wall temperatures. This is particularly salient at the cold wall since for  $T_h = 1300$  K and  $T_c = 1100$  K the slope of the error propagation concerning the bulk temperature is almost as steep as the one concerning the wall temperature.

**Table 6**

List of the tested cases in Figure 7.

$T_h$ [K]	$T_c$ [K]	$T_b$ [K]	$T_b/T_c$
700	500	350	0.70
900	700	550	0.79
1100	900	750	0.83
1300	1100	950	0.86

## 4. Propagation of temperature uncertainties

In this section, the propagation of the temperature uncertainties on the wall heat fluxes is analyzed with two methods. The computation of the propagation of uncertainties using the GUM method is compared to the results obtained by the direct computation of heat fluxes with altered temperature values. The uncertainty associated with the thermal conductivity has almost no influence on the results. It is then, neglected to simplify the equation. The uncertainties on the input variables are assumed to be uncorrelated. In the following, we consider the uncertainty of measurements on one parameter at a time and we only investigate the uncertainties relative to temperature.

### 4.1. Symmetric heating conditions

In the symmetric heating case, the Taylor series expansion of the simplified heat transfer correlation proposed by David *et al.* [27] is computed. The expression of the uncertainty propagation is given by:

$$\frac{\Delta\phi_{\text{sym}}}{\phi_{\text{sym}}} = \sqrt{A_{\text{sym}}^2 + B_{\text{sym}}^2 + C_{\text{sym}}^2 + D_{\text{sym}}^2}, \quad (7)$$

with

$$\begin{aligned} A_{\text{sym}} &= \Delta\text{Re}_b \left( \frac{0.8}{\text{Re}_b} \right), \\ B_{\text{sym}} &= \Delta\text{Pr}_b \left( \frac{0.4}{\text{Pr}_b} \right), \\ C_{\text{sym}} &= \Delta T_b \left( \frac{0.9}{T_b} - \frac{1}{T_w - T_b} \right), \\ D_{\text{sym}} &= \Delta T_w \left( -\frac{0.9}{T_w} + \frac{1}{T_w - T_b} \right). \end{aligned}$$

In Sections 4.1.1, and 4.1.2, the studied conditions are those described in Table 3, except for the bulk temperature which varies in order to cover the entire range of the correlation in terms of bulk-to-cold wall temperature ratio.

#### 4.1.1. Uncertainties on the measurements of the wall temperature depending on the bulk-to-wall temperature ratio

The uncertainties on the wall flux depending on the bulk-to-cold wall temperature ratio and the error of the measurements of the wall temperature are plotted

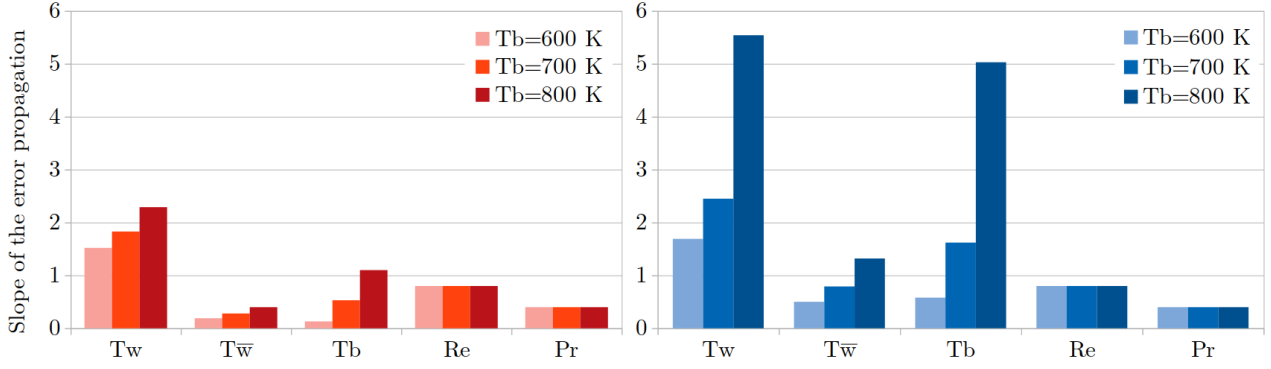


**Figure 6:** Slope of the error propagation in absolute value for the five flow parameters. Three bulk temperatures are investigated. The bulk Reynolds number is 60 000 for all the tested cases and the wall temperatures are 1300 K and 900 K.

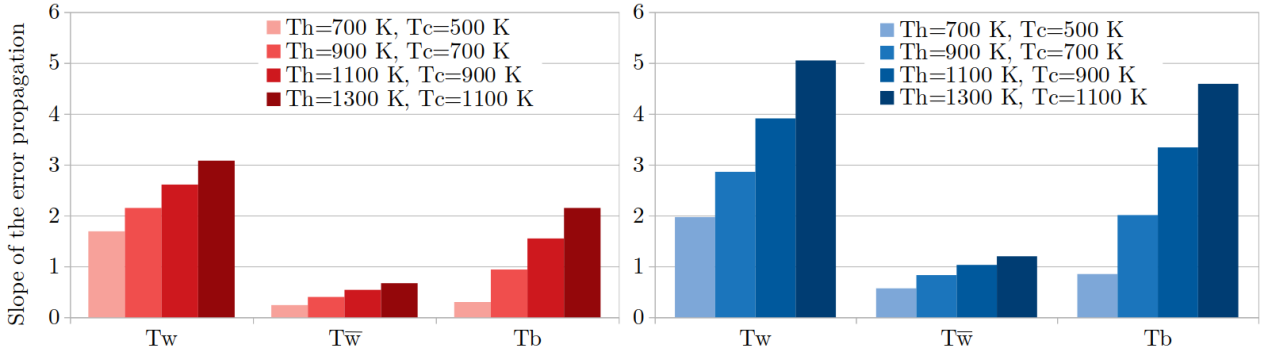


**Figure 7:** Slope of the error propagation in absolute value for wall and bulk temperatures. Four couples of wall temperatures are investigated, see Table 6. The left, respectively right, graph concerns the hot, respectively cold, wall heat flux. The bulk Reynolds number is 60 000 for all the tested cases.

in Figure 8. The top-left corner of the left graph is colored in black because, in this region, the altered cold wall temperature induces a bulk-to-altered wall temperature superior to 0.95 and is, then, out of the applicable domain of the correlation (even if the plotted bulk-to-reference wall temperature is inferior to 0.95). The wall heat fluxes, obtained by the direct computation of heat transfer correlation with the altered input wall temperature, are compared to the results obtained with the GUM. The reference wall heat flux errors are presented on the left side whereas the estimation provided by the GUM procedure is displayed on the right side. The results show the wall heat flux is strongly dependent on the wall temperature error of measurement. The shape of the lines indicates that the bigger the bulk temperature is, the more influential the error of measurement is. An under-estimation of the wall temperature leads to slightly higher uncertainty on the wall heat flux than an overestimation. The model provides an accurate estimation of the error on the entire validity domain of the correlation. Nevertheless, it is worth noting that the lines of isoerror predicted by the GUM are not linear. The error committed by the model increases with the inaccuracies of the measurement since it assumes the linearity of the studied function.

#### 4.1.2. Uncertainties on the measurements of the bulk temperature depending on the bulk-to-wall temperature ratio

The bulk temperature is also affected to the uncertainties of measurement. Figure 9 shows the uncertainties on the wall flux depending on the bulk-to-cold wall temperature ratio and the error of the measurements of the bulk temperature. The left graph exposes a strong asymmetric distribution of the error. Indeed, at a bulk-to-wall temperature ratio of 0.70, for the same value of uncertainty, an overestimation of 10% of the bulk temperature induces an error of 16% of the wall heat flux. An under-estimation in the same conditions leads to an error of 12%. This is due to the increase of the sensitivity of the wall heat flux to bulk temperature when the temperature difference between the wall and the fluid is low. On the right graph, the estimation of the uncertainties obtained with the Taylor expansion, does not capture this asymmetric behavior of the error propagation. However, the results obtained with the GUM procedure are satisfying since the obtained error is almost equal to the average of the under-estimation and overestimation. For small bulk-to-wall temperature ratios, *i.e.* near the entrance of the solar receiver, the wall heat flux is only slightly affected by the uncertainties

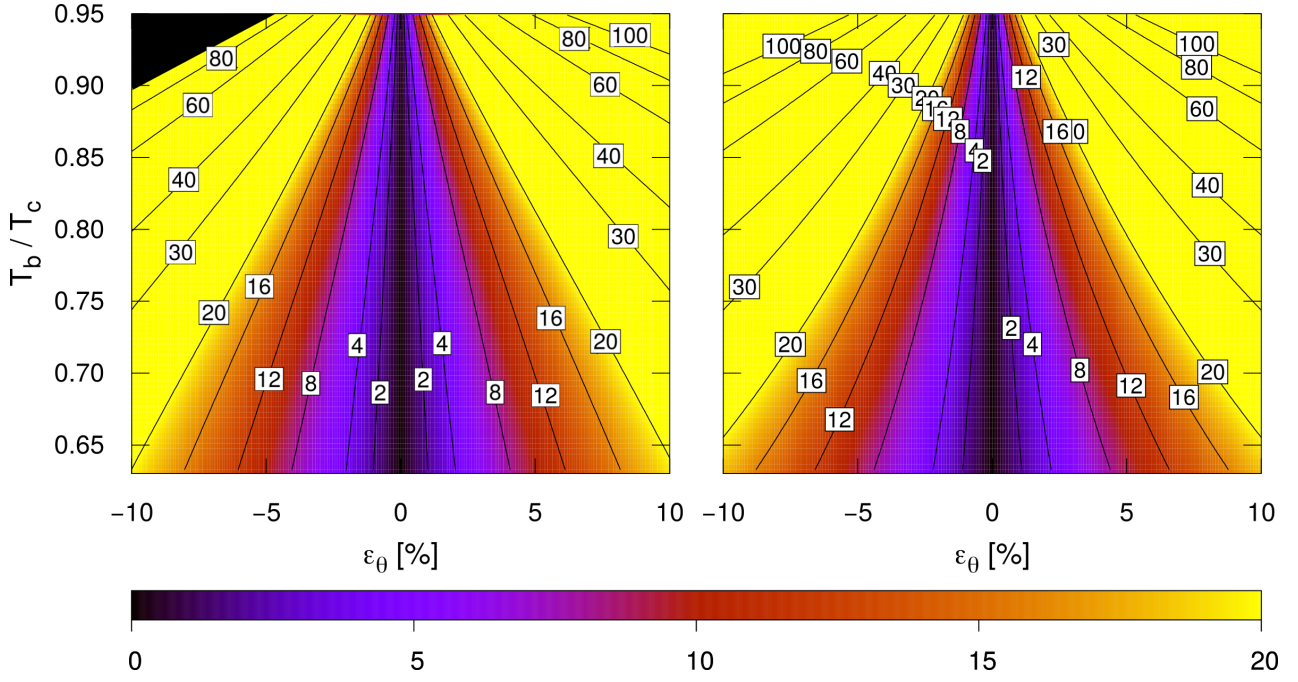


**Figure 8:** Uncertainties on the wall flux depending on the bulk-to-cold wall temperature ratio and the error of the measurements of the wall temperatures in the case of symmetric heating conditions. The left graph shows the reference results, the right graph exposes the estimation produced by the GUM. The lines indicate the isovalues of error 2%, 4%, 8%, 12%, 16%, 20%, 30%, 40%, 60%, 80% and 100%.

on the bulk temperature.

#### 4.2. Asymmetric heating conditions

Applying the Taylor series expansions to the heat transfer correlation of David *et al.* [27], the GUM provides the analytical expression of the uncertainty propagation exposed in the following equation:

$$\frac{\Delta\phi_{\text{asy}}}{\phi_{\text{asy}}} = \sqrt{A_{\text{asy}}^2 + B_{\text{asy}}^2 + C_{\text{asy}}^2 + D_{\text{asy}}^2 + E_{\text{asy}}^2}, \quad (8)$$

with

$$\begin{aligned} A_{\text{asy}} &= \Delta\text{Re}_b \left( \frac{0.8}{\text{Re}_b} \right), \\ B_{\text{asy}} &= \Delta\text{Pr}_b \left( \frac{0.4}{\text{Pr}_b} \right), \\ C_{\text{asy}} &= \Delta T_b \left( \frac{0.9}{T_b} + \frac{1.4}{T_w} \alpha (\gamma + \log(\beta)) - \frac{1}{T_w - T_b} \right), \\ D_{\text{asy}} &= \Delta T_w \left( -\frac{0.9}{T_w} \right) \\ &+ \Delta T_w \left( -1.4\alpha \frac{T_b}{T_w^2} \left( \gamma + \frac{\log(\beta)}{1 + \frac{1}{\delta} + \frac{\alpha}{\delta}} \right) + \frac{1}{T_w - T_b} \right), \\ E_{\text{asy}} &= \Delta T_{\bar{w}} \left( 2.8 \frac{T_b}{(T_w + T_{\bar{w}})^2} \log(\beta) \right). \end{aligned}$$

where  $\alpha = (T_{\bar{w}} - T_w) / (T_w + T_{\bar{w}})$ ,  $\beta = T_w / (T_w - T_b)$ ,  $\gamma = T_b / (T_w - T_b)$ ,  $\delta = (T_{\bar{w}} - T_w) / T_w$ . The logarithm used here is the natural logarithm.

Note that, when the wall temperatures are close, the terms associated with the uncertainties on the bulk and wall temperatures tend towards the ones obtained in the symmetric heating case. Indeed,  $(T_w - T_{\bar{w}}) \rightarrow 0$  induces  $\alpha \rightarrow 0$  and  $\delta \rightarrow 0$ .

In Sections 4.2.1, and 4.2.2, the studied conditions are those described in Table 5, except for the bulk temperature which varies in order to cover the entire range of the correlation in terms of bulk-to-cold wall temperature ratio.

##### 4.2.1. Uncertainties on the measurements of the wall temperatures depending on the location in the solar receiver

The uncertainties on the wall fluxes depending on the bulk-to-cold wall temperature ratio and the error of the measurements of the wall temperatures are exposed in Figure 10. On the hot side, the maximum error is obtained for an under-estimation of the hot wall temperature of 10% and a bulk-to-wall temperature ratio of 0.95. It reaches an error of 26%. The results obtained for an under-estimation of the wall temperature are similar to those obtained for an overestimation. The isoerror lines show that the wall heat flux is not very affected by the bulk-to-wall temperature ratio, especially for small errors of temperature measurement. The model is slightly under-estimating the results tracing the non-linearity of the studied function. The uncertainty propagation is bigger at the cold wall than at the hot wall. Furthermore, the results are more sen-

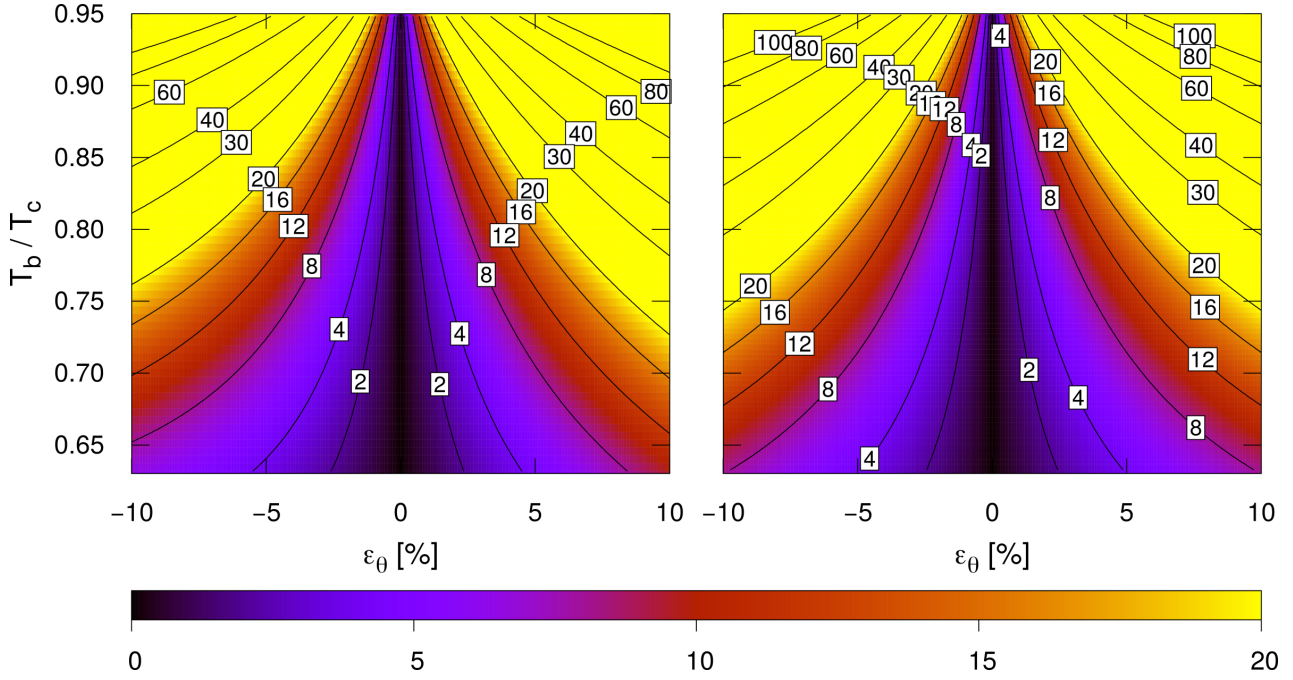


**Figure 9:** Uncertainties on the wall flux depending on the bulk-to-cold wall temperature ratio and the error of the measurements of the bulk temperature in the case of symmetric heating conditions. The left graph shows the reference results, the right graph exposes the estimation produced by the GUM. The lines indicate the isovalues of error 2%, 4%, 8%, 12%, 16%, 20%, 30%, 40%, 60%, 80% and 100%.

sitive to the bulk-to-wall temperature ratio. The uncertainty distribution is similar for under-estimation and overestimation of the wall temperature, as observed on the hot side. As for Figure 8, the results out of the applicable domain of the correlation, resulting from an under-estimation of the cold wall temperature, are masked thanks to a black triangle. It corresponds to a bulk-to-altered cold wall temperature superior to 0.95. In the case of asymmetric heating, the wall heat flux is affected by the opposite wall temperature. Figure 11 depicts the propagation of the wall temperature uncertainties on the opposed wall heat flux, *i.e.* the influence of the cold, respectively hot, wall temperature on the hot, respectively cold, wall heat flux (the black corner on the top-left graph masks the results out of the framework of the heat transfer correlation). The uncertainties on the hot wall heat flux are low since they remain below 5%. The model under-estimates the uncertainty propagation. The bottom graphs show that the cold wall heat flux is more impacted by the hot wall temperature than the hot wall heat flux by the cold wall temperature. Indeed, the errors reach 18% for the most unfavorable case. The Taylor series expansion significantly under-estimates the uncertainties when the bulk-to-cold wall temperature ratio is high (end of the solar receiver). This may be explained by the relatively strong non-linear dependence to the opposite wall temperature of the term accounting for asymmetric heating in the correlation.

#### 4.2.2. Uncertainties on the measurements of the bulk temperature depending on the location in the solar receiver

The accuracy of measurement of the bulk temperature is also impacting the wall heat flux estimation. The wall heat flux uncertainties are plotted as a function of the bulk-to-wall temperature ratio and the uncertainty of measurement of the bulk temperature in Figure 12. The results indicate that the hot wall heat flux is substantially less impacted by altered measurement of the bulk temperature than the cold wall heat flux. The GUM procedure provides a quite satisfying estimation of the uncertainties despite the non-normal distribution of the uncertainties on the wall heat fluxes. At the cold wall, an overestimation of the bulk temperature may result in a bulk-to-altered cold wall temperature ratio out of the application domain of the correlation (see the top-right corner of the bottom-left graph). For low bulk-to-cold wall temperature ratio, the uncertainty of measurement of the bulk temperature has little effect on the wall heat flux when compared to the uncertainties on the measurement of the wall (see Figure 10). However, the results are very sensitive to the bulk-to-wall temperature ratio, *i.e.* very sensitive to the location in the solar receiver: when this ratio is small, the uncertainty of measurement of the bulk temperature is not very impacting the wall heat flux. At the cold wall, when the bulk temperature is close to the cold wall temperature, the heat flux uncertainties become very high even for uncertainties of measurements

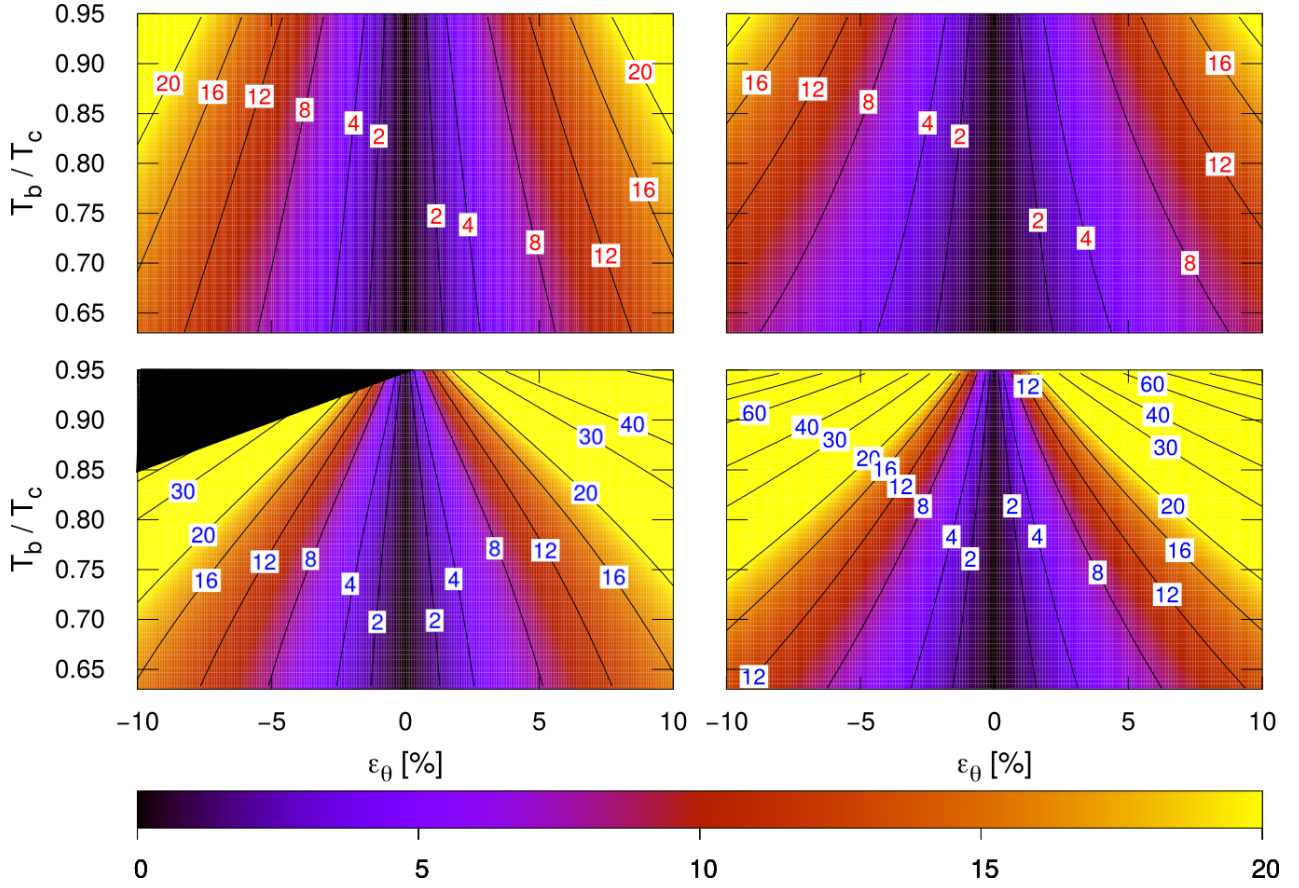


**Figure 10:** Uncertainties on the wall fluxes depending on the bulk-to-cold wall temperature ratio and the error of the measurements of the wall temperatures in the case of asymmetric heating conditions. The left graphs show the reference results, the right graphs expose the estimations produced by the GUM. The results regarding the hot, respectively cold, wall heat flux are displayed on the two top, respectively bottom, graphs. The lines indicate the isovalues of error 2%, 4%, 8%, 12%, 16%, 20%, 30%, 40%, 60%, 80% and 100%.

below 5%. Note that these high uncertainties should be put into perspective with the relatively small wall heat flux associated.

### 4.3. Comparison of the uncertainties in both types of heating

The results presented in Subsections 4.1 and 4.2 show that, contrarily to what one might think, the biggest uncertainties are obtained in the case of symmetric heating. Reducing the wall temperature difference induces a more homogeneous uncertainty propagation on the wall heat fluxes but the propagation is amplified when compared to the case of asymmetric heating. Indeed, the term accounting for asymmetric heating,  $(T_w/(T_w - T_b))^{1.4(1-(T_w/T_m))T_b/T_w}$ , balances the effect of the term  $(T_w/T_b)^{-0.9}$ . The result is a mitigation of the wall heat flux dependence to wall and bulk temperature estimation under asymmetrical heating conditions.

## 5. Conclusion

In this study, the correlation proposed by David *et al.* [27] for asymmetrically heated turbulent channel flow has been used to investigate the sensitivity to flow parameters of the wall heat fluxes and the propagation of uncertainties depending on the location in the solar receiver.

The results obtained following the Guide to the expression of Uncertainty in Measurement, which used Taylor series expansion to provide an analytical expression of the uncertainty propagation, have been compared to the results obtained with the direct computation of the heat flux with altered flow parameters. The results presented in this study show that a low bulk-to-wall temperature ratio mitigates the influence of the bulk and wall temperatures on the wall heat fluxes. In the studied conditions, the impact of the bulk temperature on the wall heat fluxes is more influenced by the working condition than the wall temperatures. Progressing in the solar receiver, the fluid temperature becomes closer to the wall temperatures. For relatively high values of the bulk-to-cold wall temperature ratio,

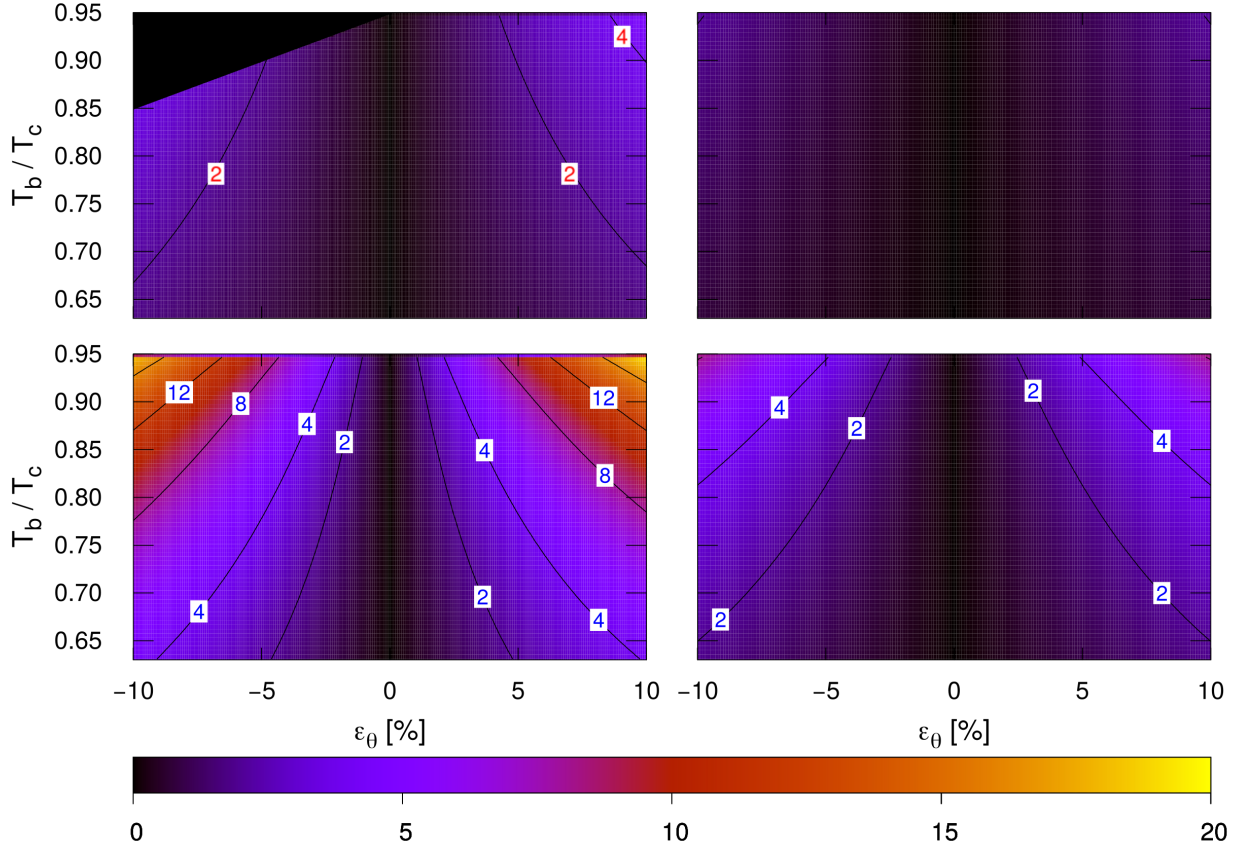


**Figure 11:** Uncertainties on the wall fluxes depending on the bulk-to-cold wall temperature ratio and the error of the measurements of the opposed wall temperatures in the case of asymmetric heating conditions. The left graphs show the reference results, the right graphs expose the estimations produced by the GUM. The results regarding the hot, respectively cold, wall heat flux are displayed on the two top, respectively bottom, graphs. The lines indicate the isovalues of error 2%, 4%, 8%, 12%, 16%, 20%, 30%, 40%, 60%, 80% and 100%.

the uncertainties on the bulk temperature become more influential than the uncertainties on the wall temperatures and are highly impacting the wall heat flux estimation. This means that it is possible to adapt the accuracy of measurement devices according to their location in the solar receiver.

A precise analysis shows that the asymmetric term induces a highly non-linear dependence of the wall heat flux to the bulk, wall, and opposite wall temperatures. In the case of inaccuracies in the measurement of the bulk temperature, the uncertainties on the wall heat flux are strongly asymmetrically distributed with regards to the 0% uncertainty line.

The expression of the heat transfer correlation used for asymmetric heating conditions involves an additional term to reproduce the heat transfers at both walls taking into account the respective effects of one on this other. Contrarily to what one might think, this new term tends to mitigate the wall heat flux dependence to bulk temperature estimation. The result is a lower wall heat flux sensitivity to wall and bulk temperatures in the case of asymmetric heating than in the

case of symmetric heating.

The method described in the GUM gives very satisfying results in the studied symmetric heating conditions. Even though the effects of the opposite wall temperature on the wall heat flux are underestimated, the method produces quite accurate estimations in the asymmetric heating case.

## 6. Acknowledgements

This work was granted access to the HPC resources of CINES under the allocation 2020-A0082A05099 made by GENCI. The authors acknowledge PRACE for awarding them access to Joliot-Curie at GENCI@CEA, France (PRACE Project : 2020225398). The authors gratefully acknowledge the CEA for the development of the TRUST platform. The authors gratefully acknowledge the Occitania region for their funding of the thesis grant.

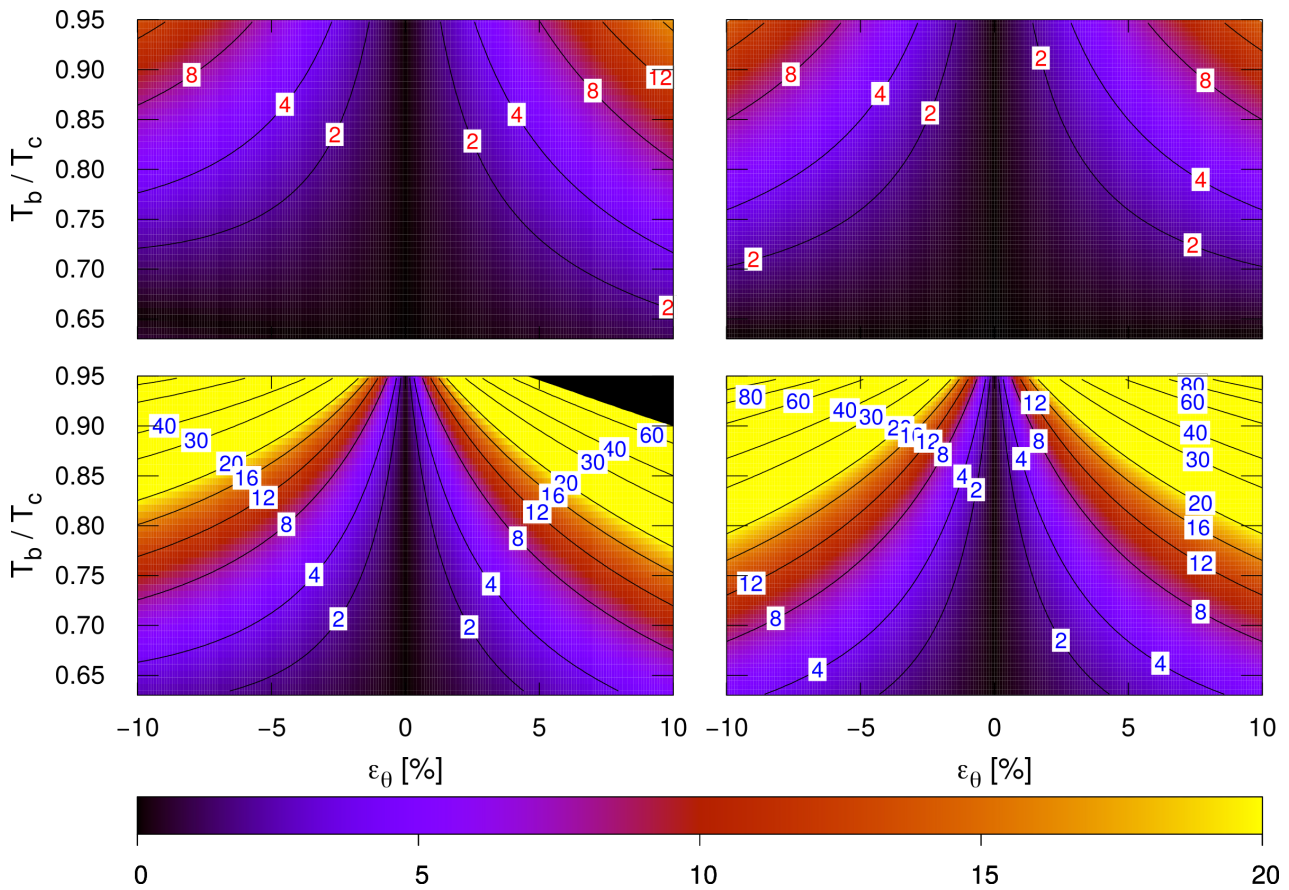


**Figure 12:** Uncertainties on the wall fluxes depending on the bulk-to-cold wall temperature ratio and the error of the measurements of the bulk temperature in the case of asymmetric heating conditions. The left graphs show the reference results, the right graphs expose the estimations produced by the GUM. The results regarding the hot, respectively cold, wall heat flux are displayed on the two top, respectively bottom, graphs. The lines indicate the isovalues of error 2%, 4%, 8%, 12%, 16%, 20%, 30%, 40%, 60%, 80% and 100%.

## CRedit authorship contribution statement

**Martin David:** Data acquisition, Writing. **Adrien Toutant:** Work guiding, Reviewing. **Françoise Bataille:** Work guiding, Reviewing.

## References

- [1] JCGM. Evaluation of measurement data – Guide to the expression of uncertainty in measurement. <https://www.bipm.org/en/publications/guides/gum.html>, 2008.
- [2] J Han, S Dutta, and S. V Ekkad. *Gas Turbine Heat Transfer and Cooling Technology*. CRC Press - Taylor & Francis Group, 2012. ISBN 978-0-429-10711-5.
- [3] Todd A. Oliver, Nicholas Malaya, Rhys Ulerich, and Robert D. Moser. Estimating uncertainties in statistics computed from direct numerical simulation. *Physics of Fluids*, 26(3):035101, 2014. ISSN 1070-6631.
- [4] Tyrone Phillips and Christopher Roy. Richardson Extrapolation-Based Discretization Uncertainty Estimation for Computational Fluid Dynamics. *Journal of Fluids Engineering*, 136:121401, 2014.
- [5] Mauro Carnevale, Francesco Montomoli, Antonio D’Ammaro, Simone Salvadori, and Francesco Martelli. Uncertainty Quantification: A Stochastic Method for Heat Transfer Prediction Using LES. *Journal of Turbomachinery*, 135, 2013.
- [6] Kathrin Menberg, Yeonsook Heo, and Ruchi Choudhary. Sensitivity analysis methods for building energy models: Comparing computational costs and extractable information. *Energy and Buildings*, 133:433–445, 2016. ISSN 0378-7788.
- [7] Francisco Uhía, Antonio Campo, and José Fernández-Seara. Uncertainty analysis for experimental heat transfer data obtained by the Wilson plot method: Application to condensation on horizontal plain tubes. *Thermal Science*, 17, 2013.
- [8] G. N. Coleman, J. Kim, and R. D. Moser. A numerical study of turbulent supersonic isothermal-wall channel flow. *Journal of Fluid Mechanics*, 305:159–183, 1995. ISSN 1469-7645, 0022-1120.
- [9] K. Wójs and T. Tietze. Effects of the temperature interference on the results obtained using the Wilson plot technique. *Heat and Mass Transfer*, 33(3):241–245, 1997. ISSN 1432-1181.
- [10] D. D. Clarke, V. R. Vasquez, W. B. Whiting, and M. Greiner. Sensitivity and uncertainty analysis of heat-exchanger designs to physical properties estimation. *Applied Thermal Engineering*, 21(10):993–1017, 2001. ISSN 1359-4311.
- [11] Jon C Helton. Uncertainty and sensitivity analysis techniques for use in performance assessment for radioactive

- waste disposal. *Reliability Engineering & System Safety*, 42(2):327–367, 1993. ISSN 0951-8320.
- [12] D. Rochman, W. Zwermann, S. C. van der Marck, A. J. Koning, H. Sjöstrand, P. Helgesson, and B. Krzykacz-Hausmann. Efficient Use of Monte Carlo: Uncertainty Propagation. *Nuclear Science and Engineering*, 177(3):337–349, 2014. ISSN 0029-5639.
- [13] Javier Mazo, Abdallah Tarek El Badry, Joan Carreras, Mónica Delgado, Dieter Boer, and Belen Zalba. Uncertainty propagation and sensitivity analysis of thermophysical properties of phase change materials (PCM) in the energy demand calculations of a test cell with passive latent thermal storage. *Applied Thermal Engineering*, 90:596–608, 2015. ISSN 1359-4311.
- [14] Dario Colorado, Xudong Ding, J. Alfredo Hernández, and Beatriz Alonso. Hybrid evaporator model: Analysis under uncertainty by means of Monte Carlo method. *Applied Thermal Engineering*, 43:148–152, 2012. ISSN 1359-4311.
- [15] Li Ming Zhou, Erfei Zhao, and Shuhui Ren. Interval element-free Galerkin method for uncertain mechanical problems. *Advances in Mechanical Engineering*, 10(1):1687814017737667, 2018. ISSN 1687-8140.
- [16] Tian Zhou, Jie Yuan, and Min Li. Simultaneously estimate solid- and liquid-phase thermal conductivities. *International Communications in Heat and Mass Transfer*, 119:104959, 2020. ISSN 0735-1933.
- [17] Cláudio R. Ávila da Silva Jr. and André Teófilo Beck. Efficient bounds for the Monte Carlo–Neumann solution of stochastic thermo-elasticity problems. *International Journal of Solids and Structures*, 58:136–145, 2015. ISSN 0020-7683.
- [18] Dawid Taler. Assessment of the indirect measurement uncertainty. In *Numerical Modelling and Experimental Testing of Heat Exchangers*, Studies in Systems, Decision and Control, pages 373–448. Springer International Publishing, 2019. ISBN 978-3-319-91127-4.
- [19] S. Oladyshkin and W. Nowak. Data-driven uncertainty quantification using the arbitrary polynomial chaos expansion. *Reliability Engineering & System Safety*, 106:179–190, 2012. ISSN 0951-8320.
- [20] H. Cho, D. Venturi, and G. E. Karniadakis. Karhunen–Loève expansion for multi-correlated stochastic processes. *Probabilistic Engineering Mechanics*, 34:157–167, 2013. ISSN 0266-8920.
- [21] G. J. K. Tomy and K. J. Vinoy. Neumann-Expansion-Based FEM for Uncertainty Quantification of Permittivity Variations. *IEEE Antennas and Wireless Propagation Letters*, 19(4):561–565, 2020. ISSN 1548-5757.
- [22] Andreas Håkansson. An investigation of uncertainties in determining convective heat transfer during immersion frying using the general uncertainty management framework. *Journal of Food Engineering*, 263:424–436, 2019. ISSN 0260-8774.
- [23] F. W. Dittus and L. M. K. Boelter. Heat transfer in automobile radiators of the tubular type. *International Communications in Heat and Mass Transfer*, 12(1):3–22, 1985. ISSN 0735-1933.
- [24] S. G. Penoncello. *Thermal Energy Systems : Design and Analysis*. CRC Press - Taylor & Francis Group, 2015. ISBN 978-0-429-17226-7.
- [25] Dawid Taler. Mathematical modeling and control of plate fin and tube heat exchangers. *Energy Conversion and Management*, 96:452–462, 2015. ISSN 0196-8904.
- [26] Marcin Trojan and Dawid Taler. Thermal simulation of superheaters taking into account the processes occurring on the side of the steam and flue gas. *Fuel*, 150:75–87, 2015. ISSN 0016-2361.
- [27] Martin David, Adrien Toutant, and Françoise Bataille. Numerical development of heat transfer correlation in asymmetrically heated turbulent channel flow. *International Journal of Heat and Mass Transfer*, 164:120599, 2021. ISSN 0017-9310.
- [28] E. N. Sieder and G. E. Tate. Heat Transfer and Pressure Drop of Liquids in Tubes. *Industrial & Engineering Chemistry*, 28(12):1429–1435, 1936. ISSN 0019-7866.
- [29] Jian Ma, Longjian. Li, Yanping Huang, and Xiaozhong Liu. Experimental studies on single-phase flow and heat transfer in a narrow rectangular channel. *Nuclear Engineering and Design*, 241(8):2865–2873, 2011. ISSN 0029-5493.
- [30] E. Battista and H. C. Perkins. Turbulent heat and momentum transfer in a square duct with moderate property variations. *International Journal of Heat and Mass Transfer*, 13(6):1063–1065, 1970. ISSN 0017-9310.
- [31] V. Gnielinski. On heat transfer in tubes. *International Journal of Heat and Mass Transfer*, 63:134–140, 2013. ISSN 0017-9310.
- [32] Dawid Taler. Simple power-type heat transfer correlations for turbulent pipe flow in tubes. *Journal of Thermal Science*, 26(4):339–348, 2017. ISSN 1993-033X.
- [33] E. Driscoll and D. Landrum. Uncertainty Analysis on Heat Transfer Correlations for RP-1 Fuel in Copper Tubing. *NTRS - NASA Technical Reports Server*, 2004.
- [34] Vinicius K. Scariot, Gustavo M. Hobold, and Alexandre K. da Silva. On the sensitivity to convective heat transfer correlation uncertainties in supercritical fluids. *Applied Thermal Engineering*, 145:123–132, 2018. ISSN 1359-4311.
- [35] Narjes Dimassi and Leila Dehmani. Experimental heat flux analysis of a solar wall design in Tunisia. *Journal of Building Engineering*, 8:70–80, 2016. ISSN 2352-7102.
- [36] Andrea Sciacchitano and Bernhard Wieneke. PIV uncertainty propagation. *Measurement Science and Technology*, 27(8):084006, 2016. ISSN 0957-0233.
- [37] Deepak Paudel and Simo Hostikka. Propagation of Model Uncertainty in the Stochastic Simulations of a Compartment Fire. *Fire Technology*, 55(6):2027–2054, 2019. ISSN 1572-8099.
- [38] Yatian Zhao, Chao Yan, Hongkang Liu, and Kailing Zhang. Uncertainty and sensitivity analysis of flow parameters for transition models on hypersonic flows. *International Journal of Heat and Mass Transfer*, 135:1286–1299, 2019. ISSN 0017-9310.
- [39] Wen-Qi Wang, Yu Qiu, Ming-Jia Li, Ya-Ling He, and Zedong Cheng. Coupled optical and thermal performance of a fin-like molten salt receiver for the next-generation solar power tower. *Applied Energy*, 272:115079, 2020. ISSN 0306-2619.
- [40] J Capeillère, A Toutant, G Olalde, and A Boubault. Thermo-mechanical behavior of a plate ceramic solar receiver irradiated by concentrated sunlight. *Solar Energy*, 110:174–187, 2014.
- [41] Arnaud Colleoni, Adrien Toutant, and Gabriel Olalde. Simulation of an innovative internal design of a plate solar receiver: Comparison between RANS and LES results. *Solar Energy*, 105:732–741, 2014. ISSN 0038-092X.
- [42] Qi Li, Nathan Guérin de Tourville, Igor Yadroitsev, Xigang Yuan, and Gilles Flamant. Micro-channel pressurized-air solar receiver based on compact heat exchanger concept. *Solar Energy*, 91:186–195, 2013. ISSN 0038-092X.
- [43] X. Dagueuet-Frick, A. Toutant, F. Bataille, and G. Olalde. Numerical investigation of a ceramic high-temperature pressurized-air solar receiver. *Solar Energy*, 90:164–178, 2013. ISSN 0038-092X.
- [44] D. Dupuy, A. Toutant, and F. Bataille. A posteriori tests of subgrid-scale models in an isothermal turbulent channel flow. *Physics of Fluids*, 31(4):045105, 2019. ISSN 1070-6631.
- [45] D. Dupuy, A. Toutant, and F. Bataille. A posteriori tests

- of subgrid-scale models in strongly anisothermal turbulent flows. *Physics of Fluids*, 31(6):065113, 2019. ISSN 1070-6631.
- [46] Dorian Dupuy, Adrien Toutant, and Françoise Bataille. A priori tests of subgrid-scale models in an anisothermal turbulent channel flow at low mach number. *International Journal of Thermal Sciences*, 145:105999, 2019. ISSN 1290-0729.
- [47] D. A. Nield. Forced convection in a parallel plate channel with asymmetric heating. *International Journal of Heat and Mass Transfer*, 47(25):5609–5612, 2004. ISSN 0017-9310.